



## Climatology of Espírito Santo and the Northern Campos Basin, Offshore Southeast Brazil

### Climatologia da Bacia do Espírito Santo e

### Parte Norte da Bacia de Campos, Região Offshore do Sudeste do Brasil

Claudine Pereira Dereczynski<sup>1</sup>; Ítalo dos Reis Lopes<sup>1</sup>; Natasha Oliveira de Carvalho<sup>1</sup>;  
Maria Gertrudes Alvarez Justi da Silva<sup>2</sup>; Karen Santiago Grossmann<sup>1</sup> & Renato Parkinson Martins<sup>3</sup>

<sup>1</sup> Universidade Federal do Rio de Janeiro, Instituto de Geociências, Departamento de Meteorologia,  
Av. Athos da Silveira Ramos 274, 21941-916, Rio de Janeiro, RJ, Brasil

<sup>2</sup> Universidade Estadual do Norte Fluminense, Laboratório de Meteorologia,  
Av. Alberto Lamego 2000, 28013-602, Campos dos Goytacazes, RJ, Brasil

<sup>3</sup> Petrobras, Centro de Pesquisa e Desenvolvimento Leopoldo Américo Miguez de Mello,  
Av. Horácio Macedo 950, 21941-915, Rio de Janeiro, RJ, Brasil

E-mails: claudinedereczynski@gmail.com; italoreislopes@gmail.com;

decarvalho.natasha@gmail.com; justi.meteoro@gmail.com; karen.grossmann@gmail.com; renatoparkinson@gmail.com

Recebido em: 01/11/2018 Aprovado em: 12/02/2019

DOI: [http://dx.doi.org/10.11137/2019\\_1\\_386\\_401](http://dx.doi.org/10.11137/2019_1_386_401)

## Resumo

O objetivo deste trabalho é descrever o clima da Bacia do Espírito Santo e parte norte da Bacia de Campos (Área Geográfica do Espírito Santo - AGES), localizada na Região Sudeste do Brasil. Dados observacionais, obtidos da plataforma *Floating, Production, Storage and Offloading-Brazil*, operada pela Petrobras durante o período 2004-2013, são utilizados neste trabalho. Os resultados mostram que o vento a 10 metros de altura sobre a AGES sopra predominantemente de nordeste, norte, e leste durante o ano, com intensidade moderada (entre 4,0 e 7,0 m.s<sup>-1</sup>). O vento norte é mais intenso do que o vento de quadrante sul, que ocorre durante a passagem de sistemas transientes. A velocidade média do vento depende da posição do Anticiclone Subtropical do Atlântico Sul, que influencia o gradiente de pressão à superfície sobre a área em estudo. O vento é mais fraco durante o outono; atinge uma velocidade média mensal de 5,3 m.s<sup>-1</sup> em abril e é mais intenso em setembro e janeiro (7,3 e 7,1 m.s<sup>-1</sup>, respectivamente). A pressão atmosférica ao nível médio do mar oscila entre 1012,3 hPa no verão e 1019,5 hPa no inverno; a temperatura do ar a 2 metros de altura varia entre 23,2°C em setembro e 27,4°C em março; e a umidade relativa do ar a 2 metros de altura exibe um mínimo de 72,7% em maio e um máximo de 84,2% em dezembro. Com relação à frequência de sistemas frontais, uma média de 30,2 sistemas atingem o sul da AGES a cada ano, com um máximo em setembro (3,9 sistemas) e um mínimo em fevereiro (0,8 sistema).

**Palavras-chave:** Vento; Temperatura do Ar; Pressão Atmosférica ao Nível Médio do Mar

## Abstract

The objective of this work is to describe the climate of Espírito Santo and the northern part of the Campos Basin (i.e., the Espírito Santo geographical area - ESGA), which is located in southeastern Brazil. The observed data from the *Floating, Production, Storage and Offloading-Brazil* platform, operated by Petrobras during the period 2004-2013, are used in this work. The results show that the 10-m wind over the ESGA blows predominantly from the northeast, north and east directions during the year, with moderate intensity (between 4.0 and 7.0 m s<sup>-1</sup>). The north wind is more intense than the south quadrant wind, which occurs during the passage of the transient systems. The average wind speed depends on the South Atlantic subtropical anticyclone position, which influences the surface pressure gradient over the study area. The wind is weaker during autumn; it reaches a monthly average of 5.3 m s<sup>-1</sup> in April and is stronger in September and January (7.3 and 7.1 m s<sup>-1</sup>, respectively). The mean sea level pressure oscillates between 1012.3 hPa in the summer and 1019.5 hPa in the winter; the 2-m air temperature varies between 23.2°C in September and 27.4°C in March, and the 2-m relative humidity exhibits a minimum of 72.7% in May and a maximum of 84.2% in December. With regard to the frontal systems frequency, an average of 30.2 systems reach the southern ESGA each year, with a maximum in September (3.9 systems) and a minimum in February (0.8 system).

**Keywords:** Wind; Air Temperature; Mean Sea Level Pressure

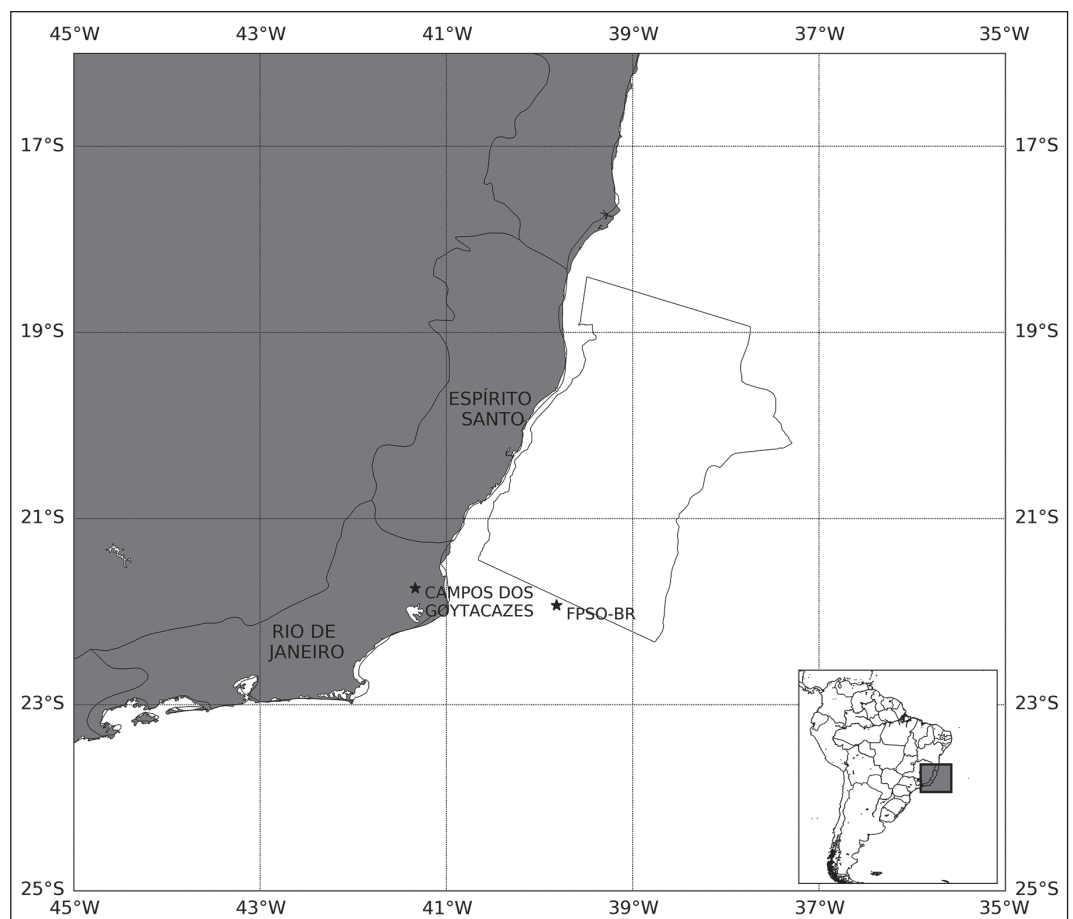
## 1 Introduction

The geographical area comprising the Espírito Santo and northern part of the Campos Basin (i.e., the Espírito Santo geographical area - ESGA) is located beneath the coastal plain in the western portion of the South Atlantic Ocean, adjacent to Espírito Santo State (southeastern Brazil) and approximately between the latitudes 22.5°S and 18.5°S and longitudes 40.5°W and 37.5°W (Figure 1). The region is economically important for Brazil since it combines fields with large productions of light oil and gas, and it has a strong contribution in supplying the national market. Thus, due to the intense oil activity in the ESGA, its climatic characterization is of extreme importance for both ocean and coastal engineering. Because meteorological conditions exert great influence on marine structures, such information is used in all phases of sea engineering enterprises and is also of great importance for environmental planning and management of the area. Therefore, the objective of this paper is to describe the ESGA climatology.

The ESGA climate is directly influenced annually by the South Atlantic subtropical anticyclone (SASA), which is a persistent large-scale high-pressure center generated by the general atmospheric circulation. The SASA, together with the South Pacific subtropical anticyclone and the Indian subtropical anticyclone, make up the Southern Hemisphere subtropical high-pressure belt established annually at approximately 35-30°S. In regions under the influence of such systems, strong subsidence and divergence of surface winds inhibit vertical movements, which generates light winds, clear skies, low relative humidity and the absence of precipitation (Seager *et al.*, 2003).

Over the ESGA, the SASA promotes stable conditions, with little cloudiness, north and east surface winds, and mild temperatures. The changes in weather are caused by the passage of transient systems, such as cold fronts, which are the most frequent synoptic systems affecting southeast Brazil through-

Figure 1  
Map of the study area, with the delimitation of the Espírito Santo Basin, which is adjacent to Espírito Santo State (southeastern Brazil). The FPSO-BR station and city of Campos dos Goytacazes in Rio de Janeiro State are indicated on the larger map.



out the year (Nobre *et al.*, 1998; Satyamurty *et al.*, 1998; Cavalcanti & Kousky, 2009; Andrade & Cavalcanti, 2018). Other meteorological systems, such as extratropical cyclones (Gan & Rao, 1991; Reboita *et al.*, 2010, 2017), subtropical cyclones (SCs) (Pinto *et al.*, 2013; Gozzo *et al.*, 2014; Reboita *et al.*, 2017; da Rocha *et al.*, 2018), squall lines (Siqueira & Marques, 2008, 2010) and inverted comma clouds (Dereczynski, 1995; Dereczynski & Hallack, 1996), are also important features to the ESGA's climate. In addition, the most striking feature of the South American tropical climate during the summer, the South Atlantic convergence zone (SACZ), also affects the ESGA. As defined by Kodama (1992), the SACZ is a cloud band over the South Atlantic, extending between the tropics and the extratropics, with a northwest-southeast tilted structure.

This paper is organized as follows: a review of the main meteorological systems affecting the ESGA, as mentioned above, is presented in Section 2. In Section 3, the data and methodology used in this work are presented. The results are discussed in Section 4, including a description of the ESGA climatology developed through the mean sea level pressure (MSLP), 10-m wind speed (10MWS) and direction (10MWD), and 2-m air temperature (2MTP) and relative humidity (2MRH). In addition, Section 4 shows the frontal systems (FSs) and frequency of occurrence for the SACZ over the ESGA. Finally, a summary of the results and the main conclusions are discussed in Section 5.

## **2 Meteorological Systems Over the ESGA: A Bibliographic Review**

Meteorological conditions over the ESGA result from the interaction of meteorological systems whose geographic and temporal extensions vary from large scale (e.g., variations in the SASA position) to the synoptic scale (including FSs, extratropical cyclones, and the SACZ) and regional scale (e.g., mesoscale convective systems (MCSs)). According to Franchito *et al.* (1998), most of the Brazilian coastal regions are influenced by the land-sea breeze circulation, which occurs due to the horizontal temperature difference between land and ocean. Although, as the land-sea breeze circulation reaches

30 km inland at most and no more than 10 km off the coast (Miguens, 2000), the ESGA, which is located 100 km from the coast, is not influenced by this local circulation.

According to the FS trajectories that penetrate South America, it is possible to distinguish the following situations: (i) systems that move from the Pacific, pass over Argentina and move towards the northeast; (ii) systems that develop over southern and southeastern Brazil, which are associated with cyclonic vortices or high levels troughs from the Pacific; (iii) systems that are organized in southern and southeastern Brazil, with intense convection associated with instability caused by the subtropical jet stream; and, finally, (iv) systems that are organized in southern Brazil resulting from frontogenesis or cyclogenesis (CPTEC/INPE, 1986).

During the winter, FSs are accompanied by air masses from high latitudes and, in some cases, they reach very low latitudes, reaching the western Amazon and the northeastern coast of Brazil. During the summer, when these systems move towards the equator, they interact with warm, humid, tropical air, producing deep, organized convection from which heavy rainfall and strong winds occur and, sometimes, precipitation occurs in the form of hail. During the summer, cold fronts are frequently positioned along the coast of Brazil, between São Paulo and Bahia, in the SACZ climatological region (Cavalcanti & Kousky 2009).

In the scientific literature, some studies present climatological surveys on the occurrence of FSs throughout the year and the various latitude bands that cover Brazil (Oliveira, 1986; Andrade, 2005; Cavalcanti & Kousky 2009; Foss *et al.*, 2016; Andrade & Cavalcanti, 2018). In summary, these systems occur throughout the year, with a maximum (minimum) frequency in spring/winter (summer). In addition, these systems advance more by the coast than within the country, and their occurrence is rare north of 20°S.

The precipitation climatology over the tropics and subtropics of South America presents a regular annual cycle. Convective activity begins in early August west of the Amazon basin and propagates to-

wards southeastern Brazil in the subsequent months. The beginning of the rainy season over southeastern Brazil occurs in the second half of October, peaking between December and February and decreasing in mid-March and early April, when the deep convective activity weakens over the tropical region. Following the annual rainfall cycle, the SACZ forms during the summer, even though there are variations in its location throughout each season, the frequency of occurrence annually, the configuration of atmospheric circulation during each occurrence and the intensity of rain and its distribution over the affected region (Cavalcanti & Kousky, 2009). Each individual SACZ episode is composed of one or several midlatitude cold fronts that intrude the subtropics and tropics, becoming stationary for a few days over southeastern Brazil (Ferreira *et al.*, 2003).

Associated with the SACZ are many severe events that result in flooding and landslides across the continent. On the other hand, during years without this system (or even its suppression), there are long periods of drought or poor distributions of rainfall over southeastern Brazil, such as those that occurred in the summers of 2014 and 2015, respectively (Coelho *et al.*, 2016). Although these characteristics have greater impact on the continent, the activities carried out across the oceans of the ESGA may be affected, such as those by the oil industry. In this sense, it is important to point out that in addition to dynamic forcing, such as wind, which acts on oil spots eventually spilled over sea and defines the overall trajectories and distributions, the action of solar radiation, with its wide wavelength spectrum, is an important factor in the chemical transformations of this oil (Garrett *et al.*, 1998). The presence of a SACZ episode for several days over an oceanic region with a significant cloud band changes the amount and spectrum of incident radiation (e.g., by changing the amount of ultraviolet radiation that reaches the surface).

Studies describing the climatology of cyclones over South America show that these systems are more frequent at high latitudes south of the ESGA. Gan & Rao (1991) and Gan (1992) recognize two preferred regions along the South American coast for the formation of cyclones: one at a latitude

of 42.5°S (San Mathias Gulf, Argentina) and the other at 32.5°S (Uruguay). In spring and autumn, both cores have approximately the same intensity of approximately 15 systems each season (5 systems/month). The Uruguay core in winter (summer) has the highest (lowest) frequency of cyclogenesis (approximately 25 (15) systems/season). In Reboita *et al.* (2010), in addition to these two regions, another center of maximum cyclogenesis also occurs, named RG1 by the author, which was located in the area between 30-20°S/50-35°W. In general, after their formation, these cyclones move to the east (southeast) when formed between 50 and 40°S (40 and 15°S), which is away from the coast (Gan & Rao 1991). In Petrobras (2012), a climatology of cyclones over the Atlantic Ocean is presented for the period 1979-2009, which was obtained with MSLP data from the Climate Forecast System Reanalysis (CFSR)/National Centers for Environmental Prediction (NCEP) at 0000, 0600, 1200 and 1800 UTC and using the CYCLOC scheme (Murray & Simmonds 1991). Their results show no record of cyclones north of 20°S. However, although no system has formed and shifted over the ESGA and despite the predominant direction of systems being towards the southeast, systems moving south of the ESGA can generate waves in the study region. For this, it is necessary that formed cyclones remain semistationary (or have very slow displacement) and continues acting for a sufficient time to produce a wave-generating track, which can reach the ESGA region.

SCs are low-pressure systems that present both extratropical and tropical structures during their development. These hybrid cyclones are nonfrontal, with a warm nucleus in the lower troposphere and a cold nucleus at high levels (Hart 2003). In Gozzo *et al.* (2014), there is a SC climatology for the period 1979-2011 over the southwestern sector of the South Atlantic basin, including the weaker and shallower systems observed mainly in the RG1 region. The results of Gozzo *et al.* (2014) indicate that the average number of SCs is 7/year, and summer is the season with the highest frequency of SCs. However, the most intense events are observed in the fall. SCs travel short distances at lower speeds than extratropical cyclones, interacting more efficiently with the unstable environment in which they develop. In



agreement with Gozzo *et al.* (2014), the RG1 region is the main subtropical cyclogenetic area over the South Atlantic Ocean.

In addition to the synoptic scale systems that affect the weather conditions over the ESGA, it is important to highlight the MCSs consisting essentially of individual nuclei or agglomerates of cumulonimbus clouds (Maddox, 1980). These systems are responsible for severe weather conditions in Brazil, such as wind gusts, heavy rainfall, lightning, thunder, precipitation in the form of hail (in some cases) and, more rarely, water spills and tornadoes (Silva Dias, 1999). Such systems can impact maritime economic activities (e.g., the operational activities of the oil industry) and, notably, the support of offshore platforms and maritime transport.

An interesting survey on MCSs observed in southeast Brazil is found in Siqueira & Marques (2008) and Siqueira & Marques (2010). In these works, by analyzing three years (1998-2000) of data from the International Satellite Cloud Climatology Project (ISCCP), the frequencies and trajectories of MCSs were determined over the region 27-16°S/49-30°W, as well as the main characteristics of these systems. The 1220 systems detected during the period were classified as having FS, nonfrontal system (NFS), continental, oceanic or coastal origins. Convective systems that appeared within two days before or two days after the passage of an FS or during the establishment of the SACZ over the region are called FSs, and the systems with origins outside this period were referred to as NFSs. The results of Siqueira & Marques (2008) are discriminated by the frequencies of MCSs in each of the groups defined above and by season. Their results show that the total number of continental systems is approximately the same as that of ocean systems, but these so-called coastal systems appear much less frequently. In the area analyzed by the authors, the continental part represents half of the oceanic area, but strong heating at the surface and in the atmosphere over the continental area favors more intense convection in that area, resulting in a substantial number of continental systems. The FS MCSs are much more frequent than those of NF origin, which is an indicator of the importance of the cold fronts in the organization of convective cloudiness over Southeast Brazil.

The comma cloud, also called a cold air vortex, is a low-pressure system in the middle and lower levels of the atmosphere with a cold core, which may sometimes form at the rear of FSs within the cold air mass. According to Rasmussen (1981), Reed & Blier (1986) and Locatelli *et al.* (1982), the typical scale of this phenomenon is meso- $\alpha$ , representing a diameter between 500 and 1500 km and duration of approximately two days. When they occur in the Southern Hemisphere, such systems are called inverted comma clouds due to their appearance in satellite images during their initial phase (Dereczynski 1995; Dereczynski & Hallack 1996). There are few papers about inverted comma clouds in South America. Dall'Antonia (1991) studied the formation of an inverted comma cloud over Paraguay and northeastern Argentina in August 1989. Bonatti & Rao (1987) investigated a case that occurred in April 1979 over Uruguay. In Dereczynski (1995), a case of an inverted comma cloud observed in June 1989 that caused strong winds in the Campos Basin was presented. Such a system was initially detected as a small cluster of convective clouds over northeastern Paraguay on 10 June 1989 and reached its mature stage in less than 42 hours. With a displacement speed of 12.5 m s<sup>-1</sup>, the system evolved and reached the Campos Basin on 12 June 1989, causing strong winds (over 20 m s<sup>-1</sup>) at Enchova station. Along the coast of southeastern Brazil, intense rainfall was observed during the passage of this system, reaching 135 mm in 24 hours over Ubatuba (SP).

In Dereczynski & Menezes (2015), hereafter DM2015, there is a climatological characterization of the Campos Basin, which is located in the Atlantic Ocean at approximately 23-21°S/42-39°W and is, therefore, adjacent to and south of the Espírito Santo Basin. It is important to emphasize that for synoptic scale purposes (i.e., a spatial scale between 200 and 2000 km and a timescale of days to one week or longer), there should be no great differences in the Campos Basin and Espírito Santo Basin climatologies since the meteorological systems affecting both regions are the same. According to DM2015, at the Campos Basin, the variation in wind intensity is small throughout the day, showing a fairly smooth maximum between 1300 and 1500 UTC and two relative minimums: the first at approximately 0900

UTC and the second at 0600 UTC. Throughout the year, the average wind intensity is lower in April and higher in September. The average winds in summer are more intense than those in winter. The direction of the wind is predominantly northeast in the four seasons. The average velocities of the north and northeast winds ( $8.0$  and  $7.3 \text{ m s}^{-1}$ , respectively) are higher than those of the winds from other directions. This characterization indicates that, in addition to the intense southwest winds (average intensity of  $6.0 \text{ m s}^{-1}$ ) from transient systems, the north and northeast winds also reach high speeds, which usually occurs before the penetration of FSs and other disturbances in the region.

DM2015 also points out that during the passage of cold fronts, the surface winds, which are originally from the northeast, turn counterclockwise towards the southwest and south, with speeds that may eventually exceed  $20 \text{ m.s}^{-1}$  (in the most intense cases). After the passage of FSs, the wind becomes southeasterly and easterly with the establishment of the SASA regime on the southeast coast of Brazil. Such a situation may persist, depending on the atmospheric conditions at a larger scale. Extratropical cyclones are transient systems that most frequently produce strong surface winds in the region, with speeds that can exceed  $20 \text{ m.s}^{-1}$  when they reach the Campos Basin.

### 3 Data and Methodology

To describe in detail the climate of a region and compare it with the climates of other global regions, the World Meteorological Organization (WMO) developed the definition of climatological normals (WMO, 1203 2017). According to the WMO, i) “averages” refers to the mean of the monthly climatological values over any specified period of time; ii) “period averages” refers to the averages of climatological data computed for any period of at least ten years starting on 1 January of a year and ending with the digit 1; iii) “normals” refers to period averages computed for a uniform and relatively long period comprising at least three consecutive ten-year periods; and iv) “climatological standard normals” refers to averages of climatological data computed for the following consecutive periods of 30 years: 1

January 1981 to 31 December 2010, 1 January 1991 to 31 December 2020, and so on. This definition was changed in the Seventeenth World Meteorological Congress (WMO, 1157 2015) by taking into consideration issues identified in The Role of Climatological Normals in a Changing Climate (WMO, 1203 2017). Therefore, instead of using nonoverlapping 30-year periods (1901-1930, 1931-1960, 1961-1990 and, in the future, 1991-2020), a “climatological standard normal” now refers to the most recent 30-year period ending in a year ending with 0 (e.g., 1981-2010 at the time of writing).

In the ESGA, the longest data series is 9 years long (i.e., that from the Floating, Production, Storage and Offloading-Brazil (FPSO-BR) platform). Thus, for climatological studies in the region, it is necessary to complement the observed data with data generated automatically by numerical modeling. The CFSR from NCEP (Saha *et al.*, 2010) was selected for use in this work because of its good spatial resolution ( $0.5^\circ$  latitude x  $0.5^\circ$  longitude) and its hourly temporal resolution. This version is used to detail the 30-year climatology (1981-2010). The summer period is considered to comprise December-January-February, autumn is March-April-May, winter is June-July-August, and spring is September-October-November. For the preparation of the seasonal averages, the summer average is always obtained starting in December of the previous year (i.e., it starts in the December 1980/January 1981/February 1981 quarter and ends in the December 2009/January 2010/February 2010 quarter).

Regarding the observational data in the study area, the meteorological station called FPSO-BR, located at  $21.93425^\circ\text{S}/39.817083^\circ\text{W}$ , is the only one used for presenting longer series of better quality compared to other stations located in the ESGA (e.g., the Plataforma de Cação 2 (PCA2), Plataforma de Peroá 1 (PPER1), FPSO Cidade de São Mateus (CDSM), and navio-plataforma Presidente Prudente de Moraes P-34), which present a maximum of 2 years of data each. The time series for the MSLP, 10MWS, 10MWD, 2MTP and 2MRH from the FPSO-BR extend from 11 October 2004 to 31 December 2013. All data series were compared among themselves and to the series extracted from

the CFSR at the grid points closest to each platform. From this evaluation, it was possible to observe that the 2MTP of the FPSO-BR was higher than that at all other platforms since January 2011 (almost 2°C warmer). Thus, it was decided to use the 2MTP data from FPSO-BR only from November 2004 to December 2010 (6 years and 2 months). In relation to the FPSO-BR 2MRH data, only the period from December 2008 to December 2013 (5 years and 1 month) was used in this work, because the data before December 2008 are visibly spurious. The other variables (MSLP, 10MWS, and 10MWD) are quite satisfactory, and their data were used for the whole period (i.e., from November 2004 to December 2013 (9 years and 2 months)).

An objective detection of FSs over the ESGA was made using the methodology proposed by Cavalcanti & Kousky (2009), with some adaptations. Initially, the hourly data series of the MSLP, 2MTP, and 10MWD were extracted from the CFSR grid point nearest to the FPSO-BR platform (22.0°S, 40.0°W). The FS detection scheme uses the following criteria: i) Decrease in the 2MTP of at least 1°C in 24 hours, ii) increase in the MSLP of at least 1 hPa in 24 hours and iii) DIR10M between 135° and 225° (wind coming from the south quadrant). Such adaptations in the Cavalcanti & Kousky (2009) methodology, using smaller thresholds, were made considering the latitudinal position of the region and the fact that the climatology is being detailed over the ocean, where the daytime amplitude of the used variables (mainly for 2MTP) is smaller than the observed amplitude over the continental surface (Ayoade, 1983). The beginning of the FS is considered when the three conditions are achieved simultaneously. After the end of the FS passage, it is computed the period (in hours) with the wind blowing from the southern quadrant.

## 4 Results

In this section, we present the ESGA climatology considering the variables MSLP, 2MTP, 2MRH, 10MWS, and 10MWD. First, a description of the seasonal fields is made from the 30-year CFSR climatology (1981-2010). Next, an analysis of the annual and diurnal cycles of the same variables is presented considering the FPSO-BR data series. Finally, the FSs and SACZ frequency of occurrence are presented.

### 4.1 Mean Sea Level Pressure (MSLP) and Surface Wind Climatologies

Figure 2 shows the MSLP and 10-m wind seasonal climatologies over the continental region and Atlantic Ocean, which is adjacent to the study area. The lowest MSLP values in the study region occur in the summer (Figure 2A; between 1013 and 1014 hPa) when the SASA center is in its southernmost position and furthest from the continent. A small low-pressure center of 1012 hPa south of the ESGA is observed at approximately 27°S/47°W. Despite the low MSLP values in the whole area during the summer, the horizontal gradient pressure is more intense than that during other seasons, and the study region is located along the western edge of the SASA, where such horizontal pressure gradients are more intense. In the figure, it is possible to observe weak winds at the center of the anticyclone, with intensification towards its boundaries. Thus, in the summer, according to the CFSR climatology, the wind reaches its maximum average intensity (5.5 m.s<sup>-1</sup>) and blows from the northeast direction.

In autumn (Figure 2B), the SASA begins to move towards the continent, and the MSLP over the ESGA increases, fluctuating between 1015 and 1016 hPa despite the weak MSLP gradients that promote weak easterly winds (3 m.s<sup>-1</sup>) in the study region, which results in the lowest intensity throughout the year. The low-pressure center south of the study area continues to appear in the fall, but with a smaller diameter and a center of 1015 hPa at approximately 26°S, 46°W. The presence of a 1016 hPa high-pressure center west of the ESGA is also observed at approximately 21°S, 44°W.

In winter (Figure 2C), the SASA center lies in its northernmost position and over the interior of the continent (28°S, 10°W), when the highest MSLP over the ESGA area is observed (between 1020 and 1021 hPa). As a result, the SASA borders the continent and, in the ESGA region, the wind speed, which is still in the eastern quadrant, increases slightly (3.5 m.s<sup>-1</sup>) in relation to that in autumn.

In the spring (Figure 2D), the pressure drops over the ESGA, oscillating between 1016 and 1017 hPa, and the pressure gradient increases again as the



SASA center moves away from the continent. The study region is located at the western edge of this system again, and the wind intensifies, reaching  $4.5 \text{ m.s}^{-1}$  and blowing from the northeast. The low-pressure center south of the study area, although it does not show closed isobars in this MSLP analysis (with a 1 hPa interval), can be noticed along the coast of Rio de Janeiro and São Paulo through the reduced MSLP in the area (1016 hPa).

Therefore, it is observed that the intensity and direction of the wind over the ESGA are directly related to the position and intensity of the SASA.

The monthly averages of the MSLP observed at the FPSO-BR station exhibit a variation of 8 hPa during the year, with a minimum in December (1011.6 hPa) and a maximum in July and August (1019.8 hPa). The lowest values are observed in the hottest months of the year, from December to March (average of 1011.9 hPa), and the highest values are observed in winter, or June-July-August (1019.5

hPa). In spring, the MSLP (1015.7 hPa) is higher than that in autumn (1014.3 hPa). Summer is the season with lowest pressure (1012.3 hPa). The daily MSLP cycle exhibits a semidiurnal tide, with two maxima at 0100 and 1300 UTC and two minima at 0700 and 1900 UTC. The 1300 UTC maximum (1016.7 hPa) is higher than the 0100 UTC maximum (1016.2 hPa), and the 1900 UTC minimum (1014.3 hPa) is lower than the 0700 UTC minimum (1014.6 hPa). We observe that the 2 hPa diurnal variability is small when compared to the observed standard deviation (5 hPa) and the annual variation (8 hPa). This persistent semidiurnal oscillation in the atmospheric tide is also clear in the hourly, monthly, annual and multiannual series (Hagan *et al.* 2003).

By comparing the 10MWS annual cycles observed at the FPSO-BR station with those observed in the Campos Basin at the Enchova, Garoupa and P-40 stations by DM2015, a very similar behavior was observed: a minimum of  $5.3 \text{ m.s}^{-1}$  in April, a main maximum of  $7.6 \text{ m.s}^{-1}$  in September and a sec-

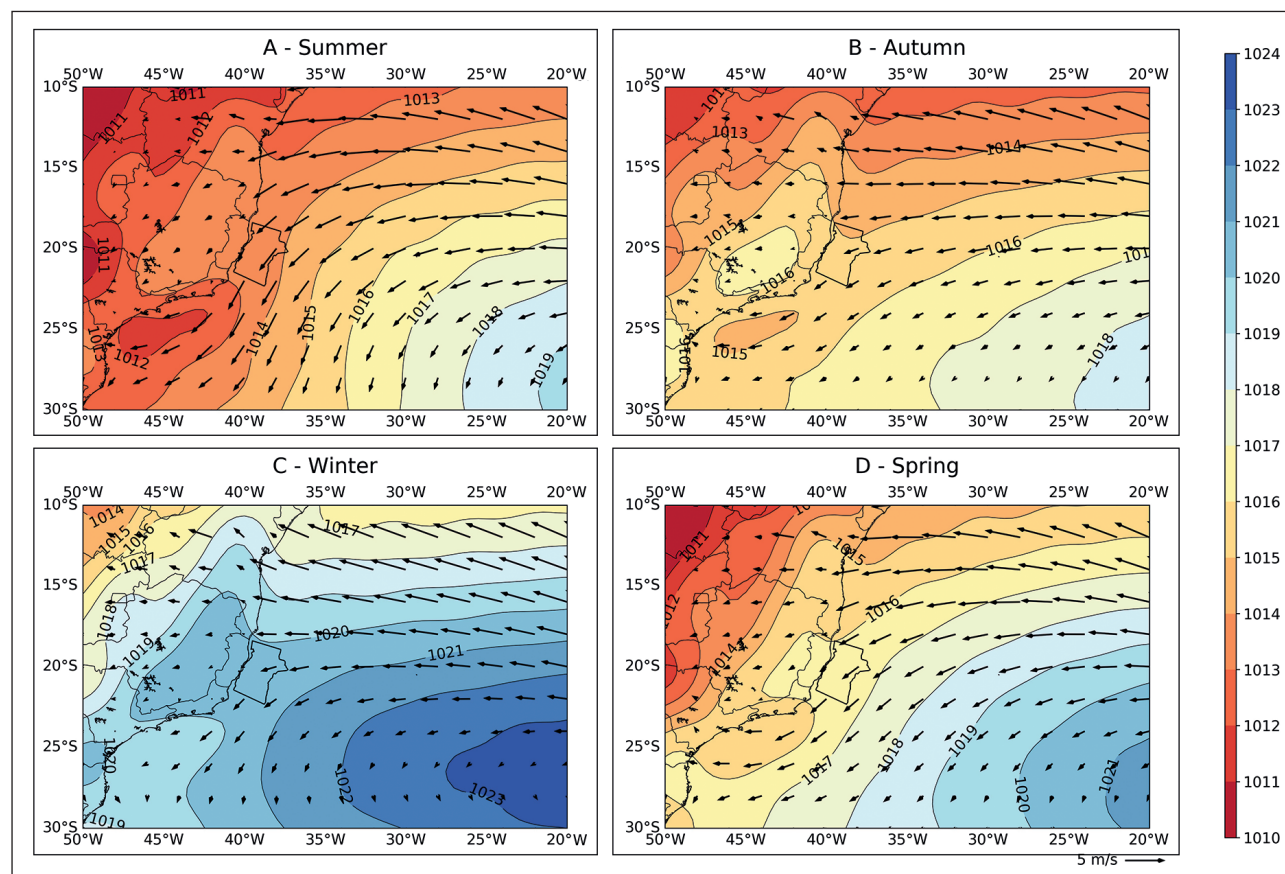


Figure 2 MSLP (hPa) and 10MWS ( $\text{m.s}^{-1}$ ) from the CFSR seasonal climatology (1981-2010): A. Summer; B. Autumn; C. Winter; D. Spring. The Espírito Santo Basin is located across the Atlantic Ocean, east of Espírito Santo State.



ondary maximum of  $7.1 \text{ m.s}^{-1}$  in January. It is, therefore, interesting to note that contrary to the CFSR spatial climatology presented in Figure 2 and from the ERA-Interim climatology (figure not shown), the highest wind velocities at the FPSO-BR station occur in spring ( $7.2 \text{ m.s}^{-1}$ ), not in summer ( $6.9 \text{ m.s}^{-1}$ ).

Regarding the 10MWS diurnal cycle, there is a slight decrease in the intensity of the wind at night until it reaches a minimum of  $5.5 \text{ m.s}^{-1}$  at 1800 UTC, when the wind rapidly intensifies until it reaches a maximum of  $6.2 \text{ m.s}^{-1}$  at 0100 UTC. This same pattern is also observed in DM2015. It is observed at the FPSO-BR station that the diurnal cycle amplitude of the 10MWS ( $0.7 \text{ m.s}^{-1}$ ) is small when compared to the annual cycle amplitude ( $2.3 \text{ m.s}^{-1}$ ).

The wind roses constructed with the same data are shown in Figure 3. Regarding the wind direction, the wind prevails from the northeast, then from the north and finally from the east during the

four seasons. In summer, due to the lower frequency of FSs, the northeast and north winds exceed 73%, while the total southwest, south and southeast directions are the least frequent (13.4%) compared to those during other seasons. West and northwest winds are not common, especially in spring, when the former occurs in only 1.26% of cases, and the second only occurs in 1.76% of cases. With respect to the magnitude of the winds, speeds between 4 and  $7 \text{ m.s}^{-1}$  are predominant during the four seasons, as well as those between 7 and  $10 \text{ m.s}^{-1}$ , except in autumn, when the second-most frequent class oscillates between 0.5 and  $4 \text{ m.s}^{-1}$ . Autumn is the season of the year with the highest occurrence of calm winds (0.51%). The classes of more intense winds (greater than or equal to  $13 \text{ m.s}^{-1}$ ) occur more (less) frequently during spring (autumn). It is interesting to note that the north wind is more intense than the south quadrant wind, which occurs during the passage of transient systems during the four seasons.

#### A - Summer

Dir/Class Wind ( $\text{m s}^{-1}$ )	0.5 - 4.0	4.0 - 7.0	7.0 - 10.0	10.0 - 13.0	13.0 - 16.0	$\geq 16.0$	Total	%	Mean ( $\text{m s}^{-1}$ )
N	526	2116	2117	736	38	0	5533	29.76	8.6
NE	1019	3741	2853	482	5	1	8101	43.58	7.7
E	627	848	127	17	1	0	1620	8.71	5.4
SE	420	486	198	24	0	0	1128	6.07	5.7
S	285	357	85	21	0	0	748	4.02	5.5
SW	263	288	62	3	0	0	616	3.31	5.1
W	243	136	15	0	0	0	394	2.12	4.3
NW	178	156	58	10	1	0	403	2.17	5.5
<b>Subtotal</b>	<b>3561</b>	<b>8128</b>	<b>5515</b>	<b>1293</b>	<b>45</b>	<b>1</b>	<b>18543</b>	<b>99.75</b>	
%	19.16	43.72	29.67	6.96	0.24	0.01			
Calm							47	0.25	
<b>Total</b>							<b>18590</b>		

#### B - Autumn

Dir/Class Wind ( $\text{m s}^{-1}$ )	0.5 - 4.0	4.0 - 7.0	7.0 - 10.0	10.0 - 13.0	13.0 - 16.0	$\geq 16.0$	Total	%	Mean ( $\text{m s}^{-1}$ )
N	882	1701	1087	173	2	0	3845	20.36	6.9
NE	1526	2306	721	47	2	0	4602	24.37	5.9
E	1403	1330	200	9	0	0	2942	15.58	4.9
SE	1007	1327	344	48	5	0	2731	14.46	5.7
S	606	1089	342	64	5	2	2108	11.16	6.2
SW	448	603	298	75	8	0	1432	7.58	6.4
W	306	139	41	13	0	0	499	2.64	4.6
NW	348	205	66	7	0	0	626	3.32	4.7
<b>Subtotal</b>	<b>6526</b>	<b>8700</b>	<b>3099</b>	<b>436</b>	<b>22</b>	<b>2</b>	<b>18785</b>	<b>99.49</b>	
%	34.56	46.08	16.41	2.31	0.12	0.01			
Calm							96	0.51	
<b>Total</b>							<b>18881</b>		

## C - Winter

Dir/Class Wind (m s <sup>-1</sup> )	0.5 - 4.0	4.0 - 7.0	7.0 - 10.0	10.0 - 13.0	13.0 - 16.0	≥ 16.0	Total	%	Mean (m s <sup>-1</sup> )
N	454	1779	1873	557	26	0	4689	25.15	8.4
NE	952	2645	1404	223	3	0	5227	28.03	7.1
E	910	1569	463	14	0	0	2956	15.85	5.9
SE	631	1078	337	24	1	0	2071	11.11	6.0
S	356	776	388	57	6	0	1583	8.49	6.8
SW	306	576	438	78	6	0	1404	7.53	7.2
W	166	93	10	2	0	0	271	1.45	4.1
NW	187	176	44	4	1	0	412	2.21	5.3
<b>Subtotal</b>	<b>3962</b>	<b>8692</b>	<b>4957</b>	<b>959</b>	<b>43</b>	<b>0</b>	<b>18613</b>	<b>99.83</b>	
%	21.25	46.62	26.59	5.14	0.23	0			
Calm							32	0.17	
<b>Total</b>							<b>18645</b>		

## D - Spring

Dir/Class Wind (m s <sup>-1</sup> )	0.5 - 4.0	4.0 - 7.0	7.0 - 10.0	10.0 - 13.0	13.0 - 16.0	≥ 16.0	Total	%	Mean (m s <sup>-1</sup> )
N	242	1125	1464	578	20	0	3429	20.44	9.0
NE	615	2312	2528	703	12	0	6170	36.78	8.4
E	587	1237	548	8	2	1	2383	14.20	6.4
SE	468	922	299	17	2	0	1708	10.18	6.1
S	304	801	396	34	3	1	1539	9.17	6.8
SW	206	401	284	111	5	0	1007	6.00	7.4
W	129	73	9	1	0	0	212	1.26	4.3
NW	119	127	44	6	0	0	296	1.76	5.6
<b>Subtotal</b>	<b>2670</b>	<b>6998</b>	<b>5572</b>	<b>1458</b>	<b>44</b>	<b>2</b>	<b>16744</b>	<b>99.80</b>	
%	15.91	41.71	33.21	8.69	0.26	0.01			
Calm							33	0.20	

Table 1 Joint occurrence frequency of wind speed (m.s<sup>-1</sup>) and wind direction at the FPSO-BR station: A. Summer; B. Autumn; C. Winter; D. Spring.

## 4.2 Surface Temperature and Relative Humidity Climatologies

In the 2MTP seasonal climatology (figure not shown), the isotherms are oriented approximately east-west, decreasing from low to high latitudes in all four seasons. In fact, the air temperature and humidity over the ESGA are directly influenced by the sea surface temperature (SST), which varies between 22 and 24°C during the winter and 26 and 28°C during the summer (Pereira *et al.*, 2005). The warm waters along the Brazilian coast act as an important heat source, warming the air near the surface and increasing the humidity. Due to the greater variation in solar radiation between low and high latitudes in winter, the thermal gradient during this season is higher

than that during the rest of the year. Temperatures in the middle of the ocean vary slightly from winter to summer when compared to the much greater variation over the continent. According to the CFSR climatology, in summer and autumn, the average values of 2MTP over the ESGA area are very similar, ranging from 25 to 27°C. During winter, temperatures are dominant between 23 and 24°C and, in spring, temperatures rise 1°C compared to those in winter, with averages of approximately 24 and 25°C in most of the ESGA, respectively.

From the FPSO-BR observed values, the 2MTP annual cycle was constructed (figure not shown). The 2MTP annual cycle over the ESGA is small (approximately 4°C) when compared to the

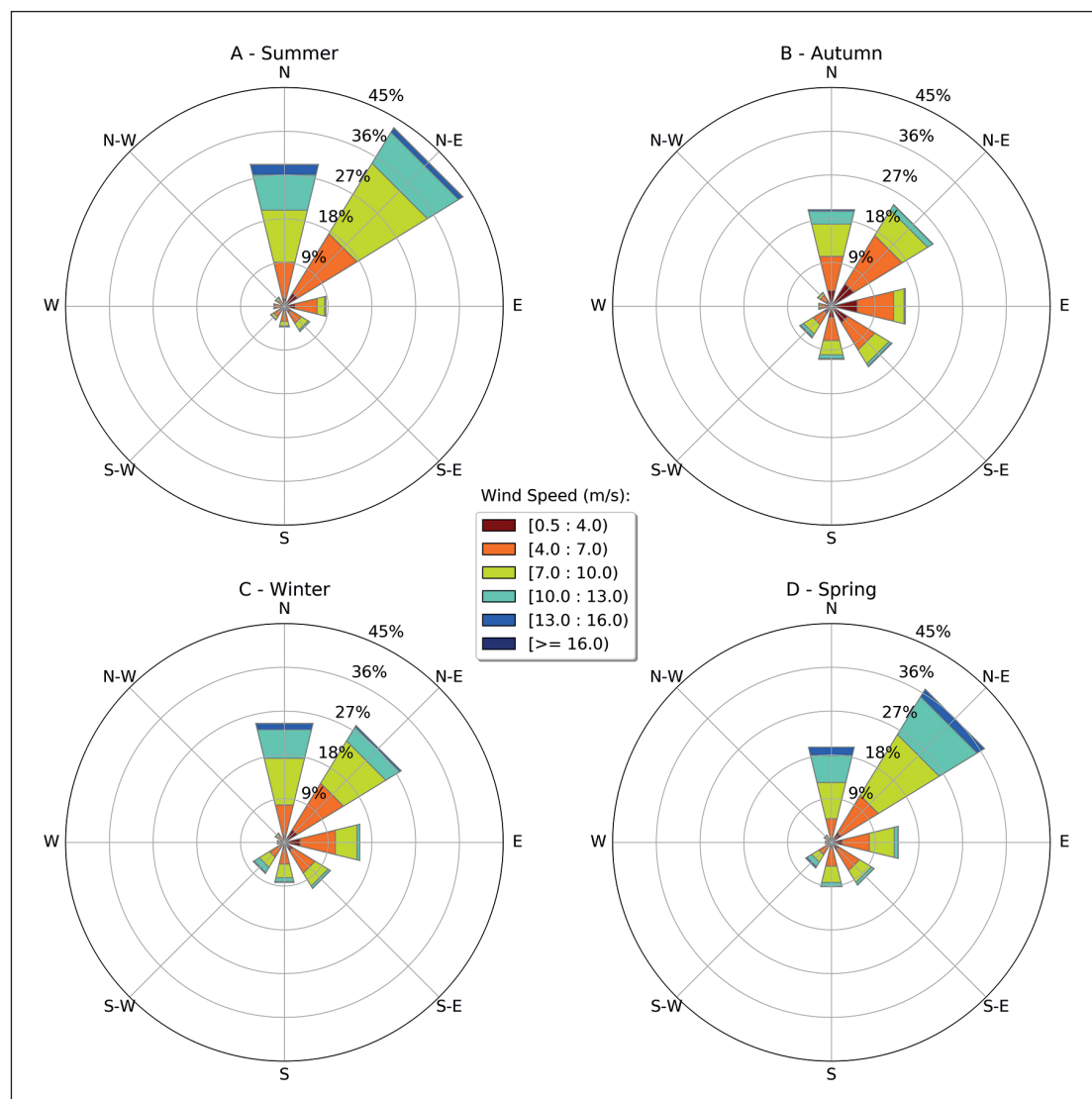


Figure 3 Wind roses. Speed ( $\text{m.s}^{-1}$ ) per wind direction at the FPSO-BR station: A Summer; B. Autumn; C. Winter; D. Spring.

annual cycle amplitudes at mid- and high latitudes, where there is great variation in the length of the day, and the Sun is not always high in the sky. In the January-February-March quarter, the 2MTP is  $27^{\circ}\text{C}$  on average, while in July-August-September, the temperature drops to  $23.3^{\circ}\text{C}$ . The hottest month is March ( $27.4^{\circ}\text{C}$ ), and the coldest month is September ( $23.2^{\circ}\text{C}$ ).

The 2MTP diurnal cycle observed at the FPSO-BR station is substantially reduced (approximately  $0.5^{\circ}\text{C}$ ), showing a minimum of  $24.8^{\circ}\text{C}$  at 0800 UTC before sunrise and a maximum of  $25.2^{\circ}\text{C}$  at approximately 1600 UTC. According to Ayoade (1983), over the oceans, the daytime temperature

range is generally less than  $0.7^{\circ}\text{C}$ , which is less than the annual amplitude. The 2MTP diurnal variation is lower on cloudy days and under calm winds than that on clear days with little cloudiness and strong winds.

The 2MRH seasonal fields constructed from the CFSR climatology (figure not shown) exhibit little variation over the ESGA throughout the year, with values ranging from 75 to 80%. In summer and spring, 2MRH exceeds 80% of the nonsignificant area while, in winter, it is below 75% in a limited portion of the ESGA.

From the 2MRH annual cycle (figure not shown) built with the FPSO-BR observed data, the



average values oscillate between 72.7% in May and 84.2% in December (annual amplitude of 11.5%), showing relative minimums in winter and relative maximums in summer. The 2MRH daily cycle (figure not shown) shows a predominance of higher mean values in the night/dawn period, with a maximum of 79.6% between 0400 and 0500 UTC, and a reduction in 2MRH with daytime heating, reaching a minimum of 75.7% between 1600 and 1700 UTC.

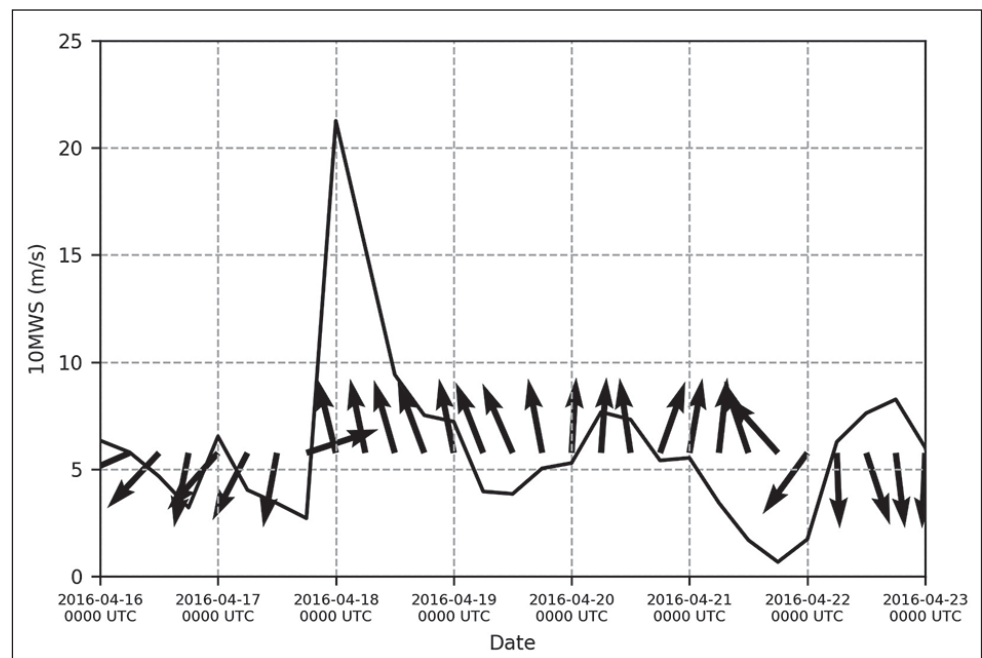
#### 4.3 Frontal System (FS) Climatology

FSs play a central role in the weather over the ESGA, producing generally strong winds, clouds, and rain. In general, one day before the passage of a cold front, the north wind intensifies. With the approach of a cold front, the wind weakens, turns counterclockwise and then begins to blow from the south. The south quadrant wind often reaches high speeds, and wind gusts are sometimes observed. After that, the wind weakens and then turns again towards the north quadrant. Figure 4 shows an example of the wind behavior at the FPSO-BR station during the cold front passage, which caused the strongest winds during the study period. According to Climanálise Bulletin/Brazilian National Institute for Space Research (CPTEC/INPE), this was the third cold front to reach Brazil during April 2006, passing through

Porto Alegre (RS) on 15 April 2006, Santos (SP) on 16 April 2006 and Campos (RJ) on 17 April 2006. Looking at Figure 4, in the beginning of the period (0600 UTC 16 April 2006), the wind was calm and blew from the north direction. With the approach of the cold front, the wind began to intensify, reaching  $8.2 \text{ m.s}^{-1}$  (direction:  $346^\circ$ ) at 1000 UTC 17 April 2006 (not shown in the figure). After that, the wind slowed down and turned counterclockwise ( $2.7 \text{ m.s}^{-1}/252^\circ$ ) at 1800 UTC 17 April 2006. From this moment, the wind began to blow from the south, reaching  $21.3 \text{ m.s}^{-1}/166^\circ$  at 0000 UTC 18 April 2006. The velocity of the south wind decreased until 1800 UTC 21 April 2006, when it turned counterclockwise and began to blow from the north quadrant again at 0000 UTC 22 April 2006.

In this work, as described in Section 2, the frequency of the FSs reaching the southern part of the ESGA is automatically computed. The results, presented in Figure 5 (light gray column), indicate an average of 0.8 to 3.9 FSs/month, totaling 30.2 systems/year. Spring is the season with the highest number of systems (3.3/month), followed by winter (3.1/month), autumn (2.4/month) and finally summer (1.2/month). Regarding the permanence of the south quadrant wind after the passage of FSs over the study area, it is estimated that it lasts for 25 hours on average.

Figure 4 10MWS ( $\text{m.s}^{-1}$ ) and direction during a cold front passage at the FPSO-BR station every 6 hours (from 0600 UTC 16 April 2006 to 0000 UTC 23 April 2006).



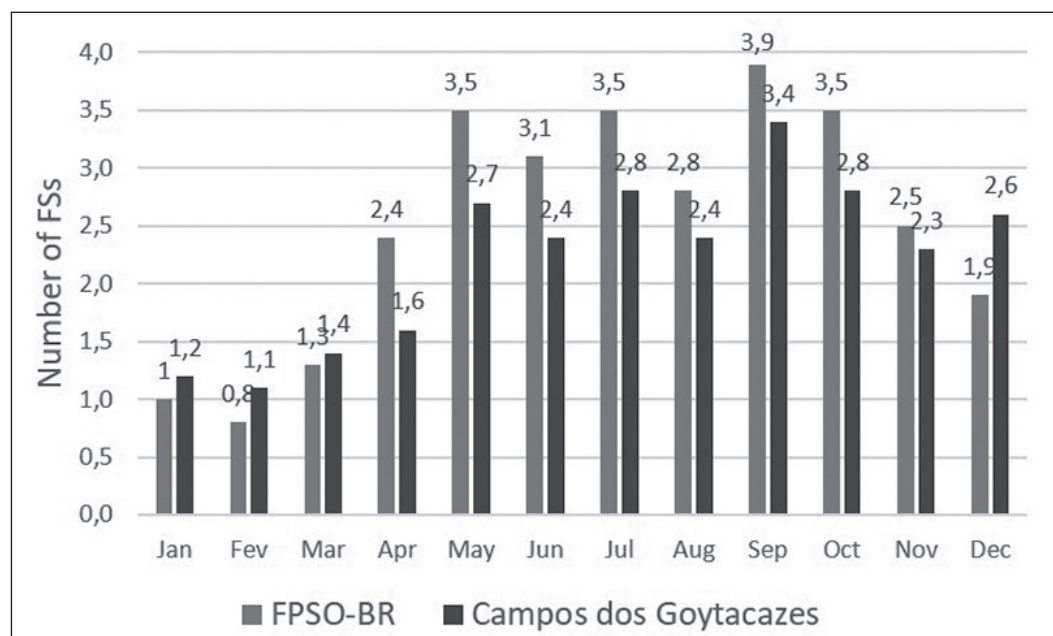


Figure 5 Monthly frequency of FSs. The light gray columns refer to the CFSR climatology at the grid point closest to the FPSO-BR station during the period 1981-2010. The dark gray columns represent the averages for the period 1996-2013 at Campos dos Goytacazes (RJ) according to the CPTEC/INPE.

For the purpose of comparison, the monthly frequency of the FSs that reached Campos dos Goytacazes (Figure 1), located in the northern State of Rio de Janeiro (slightly to the north and approximately 150 km to the west of the FPSO-BR platform), was investigated.

Such climatology was elaborated for the period 1996-2013 (18 years) considering the records of the CPTEC/INPE. The mean FS frequency at Campos dos Goytacazes was slightly lower than that obtained automatically at the FPSO-BR station. At Campos dos Goytacazes (Figure 5 – dark gray), there was a total of 26.7 systems/year, but it shows a comparable annual cycle, with the highest number of systems during spring (2.8/month), followed by winter (2.5/month), autumn (1.9/month) and finally summer (1.6/month). Therefore, we can consider the results obtained objectively in this work comparable to those observed by the operational meteorologists at CPTEC/INPE.

#### 4.4 South Atlantic Convergence Zone (SACZ) climatology

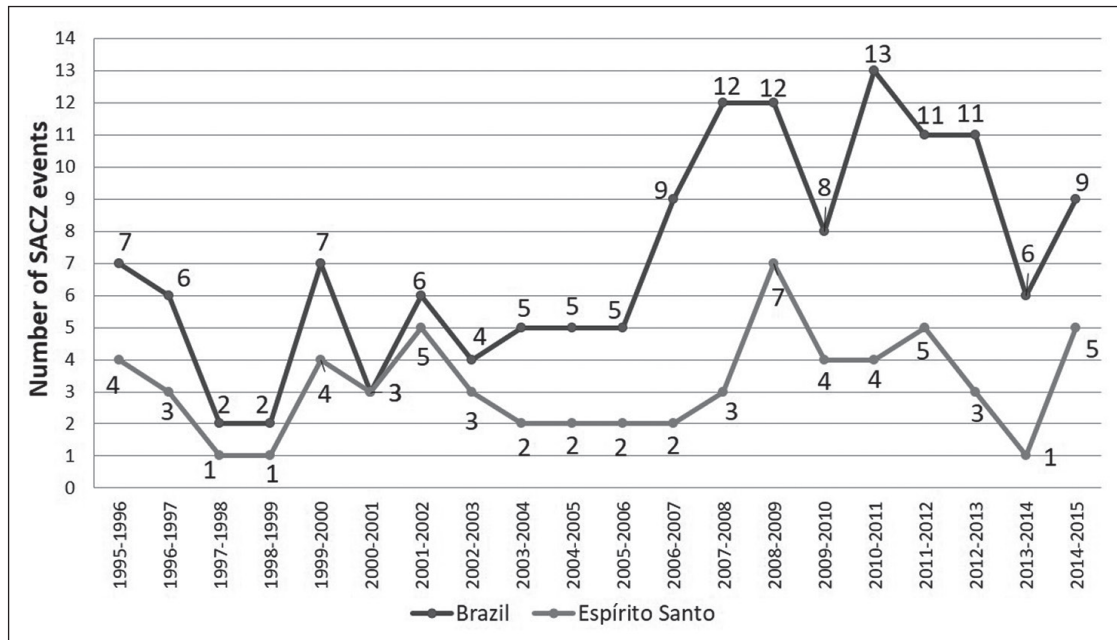
To determine the SACZ frequency of occurrence over Brazil, a survey of events was conducted considering the CPTEC. At CPTEC/INPE, the me-

teorologists register the period and location of each SACZ event monthly from October to April. For this research, the number of SACZ events over Brazil and the number of events where the SACZ axis position passes over Espírito Santo State and the adjacent coastal region were computed from October to April during 1995-2015 (Figure 6). Large interannual variability in the number of SACZ events was observed, with only 2 events occurring some years while, in others, up to 13 systems occurred. On average, 7.1 (3.2) formed over Brazil (Espírito Santo State). It is important to point out once again that a large number of SACZ events forming in a region does not guarantee a normal rainy season. During the period from October 2014 to April 2015, despite the occurrence of 9 SACZ events over southeastern Brazil, the production of rain during this period was insufficient, and a severe drought occurred, generating serious problems for industrial, agricultural and electrical generation (Coelho *et al.*, 2016).

#### 5 Conclusions

In this work, a survey of the ESGA climatology is carried out through the behaviors of the MSLP, 2MTP, 2MRH, 10MWS, and 10MWD. In addition, the FSs and SACZ frequencies of occurrence over the study area are computed.

Figure 6  
Frequency of  
SACZ events  
from Oc-  
tober to April  
(1995-2015)  
over Brazil  
(dark gray)  
and  
Espírito Santo  
State (light  
gray). Source:  
CPTEC/INPE



In the summer, warmer air and SASA displacement towards the ocean promote the decrease in the MSLP in the study area, which reaches a minimum in December. On the other hand, during this season, the horizontal pressure gradients over ESGA are intense, and the winds reach an average of  $7.1 \text{ m.s}^{-1}$ , which is slightly lower than the maximum of  $7.6 \text{ m.s}^{-1}$  reached in September. The 2MTP annual cycle lags that of the continental areas, reaching the highest monthly average in March. Additionally, in the summer, the 2MRH highest values are recorded. Autumn experiences the weakest winds, which are caused by a weak horizontal pressure gradient over the study area, with an average speed of  $5.6 \text{ m.s}^{-1}$  and a lower frequency of intense winds (greater than  $13 \text{ m.s}^{-1}$ ). In winter, the SASA intensification and penetration towards the interior of the continent and the penetration of cold air masses promote the highest MSLP values in the ESGA. Finally, in the spring, the ESGA shows the most intense winds of the year (average of  $7.2 \text{ m.s}^{-1}$  in the spring), as the SASA center again moves away from the continent, and the pressure gradient intensifies again.

The results showed that the MSLP at the FP-SO-BR station oscillates between monthly averages of 1011.6 hPa in December and 1019.8 hPa in July and August (i.e., a variation of approximately

8 hPa). The amplitude of the MSLP daytime cycle ( $2.4 \text{ hPa}$ ) is small in relation to its annual cycle, displaying an atmospheric semidiurnal tide with two maximums at 0100 UTC and 1300 UTC and two minimums at 0700 UTC and 1900 UTC. The mean 2MTP also shows a reduced diurnal cycle of approximately  $0.5^\circ\text{C}$ , with a minimum of  $24.8^\circ\text{C}$  before sunrise (0800 UTC) and a maximum of  $25.2^\circ\text{C}$  at 1600 UTC, while its annual cycle of  $4.2^\circ\text{C}$  exhibits a minimum average of  $23.2^\circ\text{C}$  in September and a maximum of  $27.4^\circ\text{C}$  in March. The monthly average 2MRH fluctuates between a minimum of 72.7% in May and a maximum of 84.2% in December, and its daily cycle is characterized by higher values during the night/dawn period (average values close to 80%) and a reduction in daytime heating, reaching a minimum (approximately 76%) between 1600 and 1700 UTC. The FPSO-BR wind is predominantly from the northeast, followed by winds from the north and east during all four seasons. The average monthly intensities are lower in the fall, reaching a minimum of  $5.3 \text{ m.s}^{-1}$  in April, and there are two highs; the main one is in September ( $7.3 \text{ m.s}^{-1}$ ), and the other is in December and January ( $7.1 \text{ m.s}^{-1}$ ). Regarding the 10MWS diurnal cycle, an amplitude of  $0.7 \text{ m.s}^{-1}$  is observed, with a slight decline in the wind intensity throughout the day starting at night (0100 UTC), when the speed reaches a maximum of  $6.2 \text{ m.s}^{-1}$ , un-



til 1800 UTC, when the wind is weaker ( $5.5 \text{ m.s}^{-1}$ ). The classes of more intense winds (greater than or equal to  $13 \text{ m.s}^{-1}$ ) occur more (less) frequently during spring (autumn). The north wind is more intense than the south quadrant wind, which occurs during the passage of transient systems during the four seasons.

Regarding the ESGA synoptic climatology, it can be observed that the highest (lowest) number of FSS occurs in September (February), with a total of 30.2 systems/year. The SACZ is a frequent summer system in southeastern Brazil, with an average of 7.1 cases observed each year during the period 1995-2015 and an average of 3.2 systems/year over the ESGA.

## 6 Acknowledgements

The authors thank Petrobras for supporting this research by means of the Research and Development Project (2014/00391-2).

## 7 References

- Andrade, K. 2005. Climatology and behavior of frontal systems over South America. PhD Thesis in Portuguese with Abstract in English. Instituto Nacional de Pesquisas Espaciais (INPE), 185p.
- Andrade, K. & Cavalcanti, I. 2018. Atmospheric characteristics that induce extreme precipitation in frontal systems over Southeastern Brazil during summer: observations and atmospheric model simulation. *International Journal of Climatology*, 38: 5368–5385. <https://doi.org/10.1002/joc.5744>
- Ayoade, J. 1983. Introduction to climatology for the tropics. John Wiley & Sons, New York, USA. 332 p.
- Bonatti, J.P. & Rao, V.B. 1987. Moist baroclinic instability in the development of North Pacific and South American intermediate-scale disturbances. *Journal of Atmospheric Sciences*, 44(18):2657-2667. [https://doi.org/10.1175/1520-0469\(1987\)044<2657:MBIITD>2.0.CO;2](https://doi.org/10.1175/1520-0469(1987)044<2657:MBIITD>2.0.CO;2)
- Cavalcanti, I. & Kousky, V. 2009. Cold fronts on Brazil. In: CAVALCANTI, I.; FERREIRA, N.; DA SILVA, M. & DIAS, M. (eds) Tempo e Clima no Brasil. Oficina de Textos, São Paulo (Brazil), p. 135-146.
- Coelho, C.A.S.; Cardoso, D.H.F. & Firpo, M.A.F. 2016. Precipitation diagnostics of an exceptionally dry event in São Paulo, Brazil. *Theoretical and Applied Climatology*, 125:769-784. <https://doi.org/10.1007/s00704-015-1540-9>
- CPTEC/INPE, 1986. Climanálise Boletim de Monitoramento e Análise Climática. Instituto Nacional de Pesquisas Espaciais. São José dos Campos, São Paulo (Brazil).
- da Rocha, R.P.; Reboita, M.S.; Gozzo, L.F.; Dutra, L.M.M. & de Jesus, E.M. 2018. Subtropical cyclones over the oceanic basins: a review. *Annals of the New York Academy of Sciences*, Special Issue: Climate Sciences REVIEW, 138-156. <https://doi.org/10.1111/nyas.13927>
- Dall'Antonia, A. 1991. Vórtice de ar frio na América do Sul - Análise diagnóstica. MSc. Thesis in Portuguese with Abstract in English, Available from the library of the São Paulo University (IAG/USP), 116p.
- Dereczynski, C. 1995. Case study of an inverted comma cloud and the subsequent occurrence of strong winds in the Campos Basin. MSc. Thesis in Portuguese with Abstract in English, Available from the library of the São Paulo University (IAG/USP), 77p.
- Dereczynski, C.P. & Hallack, R. 1996. Sistemas do tipo nuvem vírgula. In: NOBRE, C. (ed) *Climanálise. Edição comemorativa de 10 anos*. Centro de Previsão do Tempo e Estudos Climáticos (CPTEC)/ Instituto Nacional de Pesquisas Espaciais (INPE), São José dos Campos, Brazil.
- Dereczynski, C.P. & Menezes, W.F. 2015. Meteorology of the Campos Basin. In: FALCÃO, A. & FERNANDEZ, M. (eds) Regional environmental characterization of the Campos Basin. *Elsevier*, 2:1-54.
- Ferreira, R.N.; Rickenbach, T.M.; Herdies, D.L. & Carvalho, L.M.V. 2003. Variability of South American convective cloud systems and tropospheric circulation during January–March 1998 and 1999. *Monthly Weather Review*, 131:961-973. [https://doi.org/10.1175/1520-0493\(2003\)131<0961:VOSACC>2.0.CO;2](https://doi.org/10.1175/1520-0493(2003)131<0961:VOSACC>2.0.CO;2)
- Foss, M.; Chou, S.C. & Seluchi, M.E. 2016. Interaction of cold fronts with the Brazilian Plateau: a climatological analysis. *International Journal of Climatology*, 37:3644-3659. <https://doi.org/10.1002/joc.4945>
- Franchito, S.H.; Rao, V.B.; Stech, J.L. & Lorenzetti, J.A. 1998. The effect of coastal upwelling on the sea-breeze circulation at Cabo Frio, Brazil: a numerical experiment. *Anales Geophysicae*, 16:866-881. <https://doi.org/10.1007/s00585-998-0866-3>
- Gan, M. 1992. Cyclogenesis and cyclones over South America. PhD Thesis in Portuguese with Abstract in English, Instituto Nacional de Pesquisas Espaciais. INPE-5400-TDI/479, 195p.
- Gan, M.A. & Rao, V.B. 1991. Surface cyclogenesis over South America. *Monthly Weather Review*, 119:1293-1302. [https://doi.org/10.1175/15200493\(1991\)119<1293:SCOSA>2.0.CO;2](https://doi.org/10.1175/15200493(1991)119<1293:SCOSA>2.0.CO;2)
- Garrett, R.M.; Pickering, I.J.; Haith, C.E. & Prince, R.C. 1998. Photooxidation of crude oils. *Environmental Science & Technology*, 32:3719-3723. <https://doi.org/10.1021/es980201r>
- Gozzo, L.F.; da Rocha, R.P.; Reboita, M.S. & Sugahara, S. 2014. Subtropical cyclones over the Southwestern South Atlantic: climatological aspects and case study. *Journal of Climate*, 27:8543-8562. <https://doi.org/10.1175/JCLI-D-14-00149.1>
- Hagan, M.; Forbes, J. & Richmond, A. 2003. Atmospheric tides. In: HOLTON J, CURRY J, PYLE E (eds) *Encyclopedia of atmospheric sciences*, Academic Press, Cambridge, p. 159-161

- Hart, R.E. 2003. A cyclone phase space derived from thermal wind and thermal asymmetry. *Monthly Weather Review*, 131:585-616. [https://doi.org/10.1175/1520-0493\(2003\)131<0585:ACPSDF>2.0.CO;2](https://doi.org/10.1175/1520-0493(2003)131<0585:ACPSDF>2.0.CO;2)
- Kodama, Y. 1992. Large-scale common features of subtropical precipitation zones (the Baiu Frontal Zone, the SPCZ, and the SACZ) Part I: characteristics of subtropical frontal zones. *Journal of the Meteorological Society of Japan. Ser II*, 70:813-836. [https://doi.org/10.2151/jmsj1965.70.4\\_813](https://doi.org/10.2151/jmsj1965.70.4_813)
- Locatelli, J.D.; Hobbs, P.V. & Werth, J.A. 1982. Mesoscale structures of vortices in polar air streams. *Monthly Weather Review*, 110:1417-1433. [https://doi.org/10.1175/1520-0493\(1982\)110<1417:MSOVI>2.0.CO;2](https://doi.org/10.1175/1520-0493(1982)110<1417:MSOVI>2.0.CO;2)
- Maddox, R. 1980. Mesoscale convective complexes. *Bulletin American Meteorological Society*, 61:1374-1387.
- Miguens, A. 2000. Navegação: A ciência e a arte. Diretoria de Hidrografia e Navegação, Rio de Janeiro, RJ, 2100 p.
- Murray, R.J. & Simmonds, I.H. 1991. A numerical scheme for tracking cyclone centers from digital data. Part I: development and operational of the scheme. *Australian Meteorological Magazine*, 39:155-166.
- Nobre, C.; Mattos, L.; Dereczynski, C.; Tarasova, T. & Trosnikov, I. 1998. Overview of atmospheric conditions during the smoke, clouds, and radiation-Brazil (SCAR-B) field experiment. *Journal of Geophysical Research*, 103:31809-31820.
- Oliveira, A. 1986. Interactions between the South American frontal systems and the Amazonian convection. MSc. Thesis in Portuguese with Abstract in English – INPE-4008-TDL/239, Available from the Library of the Instituto Nacional de Pesquisas Espaciais, 134p.
- Pereira, C.; Santo, E. & Giarolla, E. 2005. An in situ-based climatology of the sea surface temperature field for the Southwestern Atlantic ocean and its anomalies in ENSO years. *Revista Brasileira de Meteorologia*, 20:333-346.
- Petrobras, 2012. Probability of occurrence of extratropical cyclones in the Campos and Santos Basins. Final report of the project. Available at CENPES/Petrobras.
- Pinto, J.; Reboita, M. & Da Rocha, R. 2013. Synoptic and dynamical analysis of subtropical cyclone Anita (2010) and its potential for tropical transition over the South Atlantic Ocean. *Journal of Geophysical Research: Atmospheres*, 118:10870-10883. <https://doi.org/10.1002/jgrd.50830>
- Rasmussen, E. 1981. An investigation of a polar low with a spiral cloud structure. *Journal of the Atmospheric Sciences*, 38:1785-1792. [https://doi.org/10.1175/1520-0469\(1981\)038<1785:AIOAPL>2.0.CO;2](https://doi.org/10.1175/1520-0469(1981)038<1785:AIOAPL>2.0.CO;2)
- Reboita, M.; Gan, M.; Rocha, R. & Igor, S. 2017. Surface cyclones over austral latitudes: part I - bibliographic review. *Revista Brasileira de Meteorologia*, 32:171-186
- Reboita, M.S.; da Rocha, R.P.; Ambrizzi, T. & Sugahara, S. 2010. South Atlantic ocean cyclogenesis climatology simulated by regional climate model (RegCM3). *Climate Dynamics*, 35:1331-1347. <https://doi.org/10.1007/s00382-009-0668-7>
- Reed, R. & Blier, W. 1986. A case study of comma cloud development in the Eastern Pacific. *Monthly Weather Review*, 114:1681-1695. [https://doi.org/10.1175/1520-0493\(1986\)114<1681:acsocc>2.0.co;2](https://doi.org/10.1175/1520-0493(1986)114<1681:acsocc>2.0.co;2)
- Saha, S.; Moorthi, S.; Pan, H.; Wu, X.; Wang, J.; Nadiga, S.; Tripp, P.; Kistler, R.; Woollen, J.; Behringer, D.; Liu, H.; Stokes, D.; Grumbine, R.; Gayno, G.; Wang, J.; Hou, Y.; Chuang, H.; Juang, H.H.; Sela, J.; Iredell, M.; Treadon, R.; Kleist, D.; Delst, P.V.; Keyser, D.; Derber, J.; Ek, M.; Meng, J.; Wei, H.; Yang, R.; Lord, S.; van den Dool, H.; Kumar, A.; Wang, W.; Long, C.; Chelliah, M.; Xue, Y.; Huang, B.; Schemm, J.; Ebisuzaki, W.; Lin, R.; Xie, P.; Chen, M.; Zhou, S.; Higgins, W.; Zou, C.; Liu, Q.; Chen, Y.; Han, Y.; Cucurull, L.; Reynolds, R.W.; Rutledge, G. & Goldberg, M. 2010. The NCEP climate forecast system reanalysis. *Bulletin of the American Meteorological Society*, 91:1015-1058. <https://doi.org/10.1175/2010bams3001.1>
- Satyamurty, P.; Nobre, C.A. & Dias, P.L.S. 1998. South America. In: KAROLY, D.J. & VINCET, D.G. (eds) Meteorology of the Southern Hemisphere. *Meteorological Monographs*, 27, p. 119-139.
- Seager, R.; Murtugudde, R.; Naik, N.; Clement, A.; Gordon, N. & Miller, J. 2003. Air-sea interaction and the seasonal cycle of the subtropical anticyclones. *Journal of Climate*, 16:1948-1966. [https://doi.org/10.1175/1520-0442\(2003\)016<1948:aiatse>2.0.co;2](https://doi.org/10.1175/1520-0442(2003)016<1948:aiatse>2.0.co;2)
- Silva Dias, M.A.F. 1999. Storms in Brazil. In: PIELKE, R. & PIELKE, J.R. (eds) Hazards and disasters series - Storms. Routledge. 960 p.
- Siqueira, J.R. & Marques, V.S. 2008. Occurrence frequencies and trajectories of mesoscale convective systems over southeast Brazil related to cold frontal and non-frontal incursions. *Australian Meteorological Magazine*, 57:345-357.
- Siqueira, J.R. & Marques, V.S. 2010. Structural characteristics of mesoscale convective systems over southeast Brazil related to cold frontal and non-frontal incursions. *Australian Meteorological and Oceanographic Journal*, 60:49-61. <https://doi.org/10.22499/2.6001.005>
- WMO 1157. 2015. Seventeenth World Meteorological Congress. *World Meteorological Organization*, WMO, Geneva, 695 p.
- WMO 1203. 2017. WMO guidelines on the calculation of climate normals. *World Meteorological Organization*, WMO, Geneva, 18p.